Spatial Patterns of Intrinsic Brain Activity in Mild Cognitive Impairment and Alzheimer's Disease: A Resting-State Functional MRI Study

Zhiqun Wang,[1] Chaogan Yan,[2] Cheng Zhao,[1] Zhigang Qi,[1] Weidong Zhou,[3] Jie Lu,[1] Yong He,[2]* and Kuncheng Li[1,4]*

[1]Department of Radiology, Xuanwu Hospital of Capital Medical University, Beijing 100053, China
[2]State Key Laboratory of Cognitive Neuroscience and Learning, Beijing Normal University, Beijing 100875, China
[3]Department of Neurology, Xuanwu Hospital of Capital Medical University, Beijing 100053, China
[4]Key Laboratory for Neurodegenerative Diseases, Capital Medical University, Ministry of Education, Beijing 100053, China

◆ ═══════════════════════════════════ ◆

Abstract: We used resting-state functional MRI to investigate spatial patterns of spontaneous brain activity in 22 healthy elderly subjects, as well as 16 mild cognitive impairment (MCI) and 16 Alzheimer's disease (AD) patients. The pattern of intrinsic brain activity was measured by examining the amplitude of low-frequency fluctuations (ALFF) of blood oxygen level dependent signal during rest. There were widespread ALFF differences among the three groups throughout the frontal, temporal, and parietal cortices. Both AD and MCI patients showed decreased activity mainly in the medial parietal lobe region and lentiform nucleus, while there was increased activity in the lateral temporal regions and superior frontal and parietal regions as compared with controls. Compared with MCI, the AD patients showed decreased activity in the medial prefrontal cortex and increased activity in the superior frontal gyrus and inferior and superior temporal gyri. Specifically, the most significant ALFF differences among the groups appeared in the posterior cingulate cortex, with a reduced pattern of activity when comparing healthy controls, MCI, and AD patients. Additionally, we also showed that the regions with ALFF changes had significant correlations with the cognitive performance of patients as measured by mini-mental state examination scores. Finally, while taking gray matter volume as covariates, the ALFF results were approximately consistent with those without gray matter correction, implying that the functional analysis could not be explained by regional atrophy. Together, our results demonstrate that there is a specific pattern of ALFF in AD and MCI,

thus providing insights into biological mechanisms of the diseases. *Hum Brain Mapp 32:1720–1740, 2011.* © 2010 Wiley-Liss, Inc.

Key words: posterior cingulate cortex; resting-state; default-mode; dementia; Alzheimer's disease; mild cognitive impairment; intrinsic brain activity

INTRODUCTION

Alzheimer's disease (AD) is a progressive, neurodegenerative disease that is clinically characterized by the decline of memory and other cognitive functions. Mild cognitive impairment (MCI), the most important disease state associated with AD, refers to some level of memory loss and cognitive declines among an elderly population that does not meet the criteria for dementia. It has been reported that about 10–15% of individuals presenting with MCI progress to develop dementia annually. Previous functional brain imaging studies with positron emission tomography and single-photon emission computerized tomography have demonstrated that AD and/or MCI subjects exhibit abnormally low resting cerebral blood flow and a decreased cerebral metabolic rate for glucose in the posterior cingulate, temporal, parietal, and prefrontal cortex [Bokde et al., 2001; de Leon et al., 2001; Herholz et al., 2002; Salmon et al., 2000]. In this study, we report altered patterns of intrinsic or spontaneous brain activity in both AD and MCI affected individuals using resting-state functional magnetic resonance imaging (fMRI).

Using resting fMRI, Biswal et al. [1995] were the first to demonstrate that spontaneous low-frequency fluctuations (LFFs; <0.08 Hz) of the blood oxygen level dependent (BOLD) signal during rest were of physiological importance. It was suggested that regional spontaneous BOLD fluctuations likely reflect spontaneous neuronal activity [Biswal et al., 1995; Fransson, 2005; Kiviniemi et al., 2000]. So far, this resting-state fMRI approach has been widely applied to the examination of various neuropsychiatric diseases such as multiple sclerosis [Lowe et al., 2002], attention deficit hyperactivity disorder [Castellanos et al., 2008; Tian et al., 2006; Zang et al., 2007], schizophrenia [Garrity et al., 2007; Hoptman et al., 2010; Liang et al., 2006], and major depression [Anand et al., 2005; Greicius et al., 2007]. For a comprehensive review of resting-state fMRI, see Fox and Raichle [2007] and Greicius [2008]. Recently, this technique has been used to investigate the intrinsic or spontaneous brain activity in subjects with AD or MCI [Bai et al., 2008; Greicius et al., 2004; He et al., 2007; Li et al., 2002; Maxim et al., 2005; Sorg et al., 2007; Wang et al., 2006, 2007; Zhang et al., 2009].

Resting-State fMRI Studies in AD

In one of the first studies of resting-state fMRI in AD patients, Li et al. [2002] reported significantly decreased functional synchrony of spontaneous LFFs in the hippocampus and found they decreased remarkably in AD patients. Abnormalities of regional LFFs in AD patients were also found in other brain regions such as the medial and lateral temporal lobes [Maxim et al., 2005], as well as the medial parietal lobe, including the posterior cingulate cortex/precuneus (PCC/PCu) [He et al., 2007]. Using regions of interest (ROIs) based methods, several groups have reported reduced functional integrity related to the hippocampus [Allen et al., 2007; Wang et al., 2006], prefrontal regions [Wang et al., 2007], and PCC [Zhang et al., 2009] in AD patients. Using independent component analysis (ICA), Greicius et al. [2004] showed an AD-related reduction of spontaneous brain activity within a default-mode network including the PCC and medial prefrontal cortex (MPFC).

Resting-State fMRI Studies in MCI

To the best of our knowledge, there have only been three resting-state fMRI studies examining intrinsic brain activity in MCI. Li et al. [2002] were the first to report the abnormalities of intrinsic functional activity in MCI subjects. They observed a general pattern of the LFFs in the hippocampus of healthy elderly, MCI and AD subjects (healthy elderly > MCI > AD). Recently, Bai et al. [2008] found reduced PCC LFFs in MCI patients as compared with controls. Using ICA, Sorg et al. [2007] showed eight spatially consistent resting-state brain networks, and found the default-mode areas (e.g., PCC/PCu and MPFC) had markedly reduced LFFs in MCI patients. Despite fewer studies, the findings examining subjects affected by MCI are highly consistent with those of previous AD studies [Greicius et al., 2004; He et al., 2007].

Resting-state fMRI studies have provided valuable insights into the pathophysiology of AD and MCI. However, only one study has compared the patterns of intrinsic brain activity between AD and MCI subjects [Li et al., 2002], and it focused exclusively on the hippocampus. Thus, differences in the patterns of intrinsic or spontaneous brain activity between AD and MCI across the whole cortex are still poorly understood.

Here, we investigated AD and MCI-related changes in intrinsic or spontaneous brain activity by examining the regional amplitude of low-frequency BOLD fluctuations across the whole cortex. Zang et al. [2007] proposed the use of the amplitude of low frequency fluctuations (ALFF) obtained by calculating the square root of the power spectrum in a frequency range (usually 0.01–0.08 Hz) to assess the amplitude of resting-state spontaneous brain activity. Several recent resting fMRI studies in healthy subjects

TABLE I. Characteristics of the AD, MCI patients and healthy controls

Characteristics	AD	MCI	Controls	P value
N (M/F)	16 (8/8)	16 (7/9)	22 (7/15)	0.51[a]
Age, years	69.56 ± 7.65	69.38 ± 7.00	66.55 ± 7.67	0.38[b]
Education, years	10.06 ± 3.39	10.94 ± 3.40	10.00 ± 3.93	0.70[b]
MMSE	18.50 ± 3.24	26.50 ± 1.03	28.59 ± 0.59	<0.01[b]

MMSE, mini-mental state examination; plus-minus values are means ± S.D.
[a]The P value for gender distribution in the three groups was obtained by chi-square test.
[b]The P values were obtained by one-way analysis of variance tests.

have shown that the ALFF was able to represent different physiological states of the brain [Hoptman et al., 2010; Lui et al., 2009; Yan et al., 2009; Yang et al., 2007]. In addition, He et al. [2007] recently used a limited ROI approach to show abnormal spontaneous LFFs in the PCC of AD patients. In this study, we sought to determine the characteristic patterns of ALFF changes in both early-stage AD and MCI compared with controls, as well as the differences in ALFF between AD and MCI. Given that MCI is in the preclinical stage of AD and many previous studies have commonly reported reduced spontaneous PCC activity in both AD and MCI [Bai et al., 2008; Greicius et al., 2004; He et al., 2007; Sorg et al., 2007; Zhang et al., 2009], we hypothesized that ALFF changes within the PCC would also follow a general pattern of $ALFF_{AD} < ALFF_{MCI} < ALFF_{Healthy\ elderly}$. In addition, we also expected to find AD- or MCI-related ALFF changes in other brain regions.

MATERIALS AND METHODS

Subjects

Sixty-one right-handed subjects (19 AD, 18 MCI patients, and 24 healthy elderly) participated in this study after giving written informed consent. The AD and MCI subjects were recruited from patients who had consulted a memory clinic for memory complaints at Xuanwu Hospital, Beijing, China. The healthy elderly controls were recruited from the local community by advertisements. This study was approved by the Medical Research Ethics Committee of Xuanwu Hospital.

All AD patients underwent a complete physical and neurological examination, standard laboratory tests, and an extensive battery of neuropsychological assessments. The diagnosis of AD fulfilled the Diagnostic and Statistical Manual of Mental Disorders 4th Edition criteria for dementia [American Psychiatric Association, 1994], and the National Institute of Neurological and Communicative Disorders and Stroke/Alzheimer Disease and Related Disorders Association (NINCDS-ADRDA) criteria for possible or probable AD [McKhann et al., 1984]. The subjects were assessed with the Clinical Dementia Rating (CDR) score [Morris, 1993] as being in the early-stages of AD (7 patients with CDR = 1 and 12 patients with CDR = 0.5).

Participants with MCI had memory impairment but did not meet the criteria for dementia. The criteria for identifi-

cation and classification of subjects with MCI [Petersen et al., 1999] were the following: (a) impaired memory performance on a normalized objective verbal memory delayed-recall test; (b) recent history of symptomatic worsening in memory; (c) normal or near-normal performance on global cognitive tests, including Mini-Mental State Examination (MMSE) score >24, as well as on activities described in a daily living scale; (d) global rating of 0.5 on the CDR Scale, with a score of at least 0.5 on the memory domain; (e) absence of dementia.

The criteria for healthy elderly were as follows: (1) no neurological or psychiatric disorders such as stroke, depression, epilepsy; (2) no neurological deficiencies such as visual or hearing loss; (3) no abnormal findings such as infarction or focal lesion in conventional brain MR imaging; (4) no cognitive complaints; (5) MMSE score of 28 or higher; (6) CDR score of 0.

Data from seven subjects (three AD patients, two MCI patients, and two healthy elderly) were excluded due to excessive motion (see data preprocessing). Clinical and demographic data for the remaining 54 participants are shown in Table I. There were no significant differences among the three groups in gender, age, and years of education, but the MMSE scores were significantly different ($P < 0.01$) among groups.

Data Acquisition

MRI data acquisition was performed on a SIEMENS Trio 3-Tesla scanner (Siemens, Erlangen, Germany). Foam padding and headphones were used to limit head motion and reduce scanner noise. The subjects were instructed to hold still, keep their eyes closed but not fall asleep and think of anything in particular. Functional images were collected axially by using an echo-planar imaging (EPI) sequence with the following settings: repetition time (TR)/echo time (TE)/flip angle (FA)/field of view (FOV) = 2,000 ms/40 ms/90°/24 cm, resolution = 64 × 64 matrix, slices = 28, thickness = 4 mm, voxel size = 3.75 × 3.75 × 4 mm^3, gap = 1 mm, bandwidth = 2,232 Hz/pixel. The scan lasted for 478 s. All the subjects had not fallen asleep according to a simple questionnaire after the scan. Three dimensional T1-weighted magnetization-prepared rapid gradient echo (MPRAGE) sagittal images were collected by using the following parameters: TR/TE/inversion time (TI)/FA = 1,900 ms/2.2
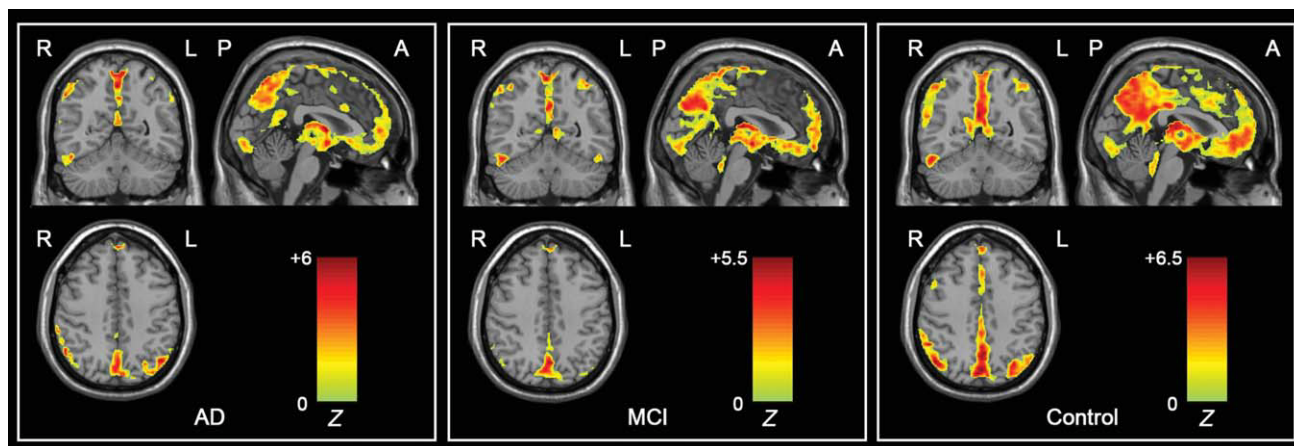
Figure 1.

Within-group ALFF maps within the AD, MCI, and healthy elderly control groups. Visual inspection indicated that the PCC and adjacent PCu had the highest ALFF values within each group and had different strengths among the three groups. The statistical threshold was set at $Z > 3.09$ ($P < 0.001$) and cluster size >189 mm^3, which corresponded to a corrected $P < 0.001$. R, right; L, left; P, posterior; A, anterior. [Color figure can be viewed in the online issue, which is available at wileyonlinelibrary.com.]

ms/900 ms/9°, resolution = 256 × 256 matrix, slices = 176, thickness = 1.0 mm, voxel size = 1 × 1 × 1 mm^3.

Data Preprocessing

Unless otherwise stated, all preprocessing were carried out using Statistical Parametric Mapping (SPM5, http://www.fil.ion.ucl.ac.uk/spm) and Data Processing Assistant for Resting-State fMRI (DPARSF) [Yan and Zang, 2010]. The first 10 volumes of the functional images were discarded due to signal equilibrium and to allow the participants' adaptation to the scanning noise. All slices of the remaining 229 volumes were corrected for different acquisition times of signals by shifting the signal measured in each slice relative to the acquisition of the slice acquired in the middle time of each TR. Then the time-series of images of each subject were motion-corrected using a least squares approach and a six-parameter (rigid body) linear transformation [Friston et al., 1995]. Seven subjects' data (2 AD patients with CDR = 1, one AD patient with CDR = 0.5, two MCI patients and two healthy elders) were excluded from further analysis because of excessive movement (>2 mm or 2°). The individual structural image (T1-weighted MPRAGE images) was coregistered to the mean functional image after motion correction using a linear transformation [Collignon et al., 1995]. The transformed structural images were then segmented into gray matter (GM), white matter, and cerebrospinal fluid by using a unified segmentation algorithm [Ashburner and Friston, 2005]. The motion corrected functional volumes were spatially normalized to the Montreal Neurological Institute (MNI) space and resampled to 3 mm isotropic voxels using the normalization parameters estimated during unified segmentation. After this, the functional images were spatially smoothed with a 4 mm full width at half maximum Gaussian kernel. Finally, using the Resting-State fMRI Data Analysis Toolkit (REST, http://rest.restfmri.net), linear trend subtraction and temporal filtering (0.01–0.08 Hz) were performed on the time series of each voxel to reduce the effect of low-frequency drifts and high-frequency noise [Biswal et al., 1995; Lowe et al., 1998].

ALFF Analyses

We applied REST to calculate the ALFF, which has been described in previous studies [Yang et al., 2007; Zang et al., 2007]. Briefly, the time courses were first converted to the frequency domain using a Fast Fourier Transform. The square root of the power spectrum was computed and then averaged across 0.01–0.08 Hz at each voxel. This averaged square root was taken as the ALFF. To reduce the global effects of variability across participants, as done in many PET studies [Raichle et al., 2001], the ALFF of each voxel was divided by the global mean ALFF value for each subject, resulting in a relative ALFF. The global mean ALFF value was calculated for each participant within a group GM mask obtained by selecting a threshold of 0.2 on the mean GM map of all 54 subjects. The relative ALFF value in a given voxel reflects the degree of its raw ALFF value relative to the average ALFF value of the whole brain.

Statistical Analyses

Within-group ALFF analysis

To explore the within-group ALFF patterns, one-sample *t*-tests (within the group GM mask) were performed on the individual ALFF maps in a voxel-wise way for each

group. The within-group statistical threshold was set at $Z > 3.09$ ($P < 0.001$) and cluster size >189 mm^3, which corresponded to a corrected $P < 0.001$. This correction was confined within the group GM mask (size: 1,575,720 mm^3) and was determined by Monte Carlo simulations [Ledberg et al., 1998] using the AFNI AlphaSim program (http://afni.nih.gov/afni/docpdf/AlphaSim.pdf).

Between-group ALFF analysis

To determine the ALFF differences among the three groups, a one-way analysis of variance (ANOVA) was performed at each voxel (within the group GM mask). To examine the between-group ALFF differences, two sample *t*-tests were further performed between every pair of the three groups on individual ALFF maps. The statistical threshold was set at $|Z| > 1.96$ ($P < 0.05$) and cluster size $>1,404$ mm^3 (search volume: 1,575,720 mm^3), which corresponded to a corrected $P < 0.05$. Likewise, the corrections were conducted using Monte Carlo simulations in AFNI.

Correlation analysis of ALFF and MMSE

To investigate the relationship between the ALFF and cognitive performance in the patients, we computed the Pearson's correlation coefficients between the ALFF and MMSE scores in the combined AD and MCI groups in a voxel-wise way. The statistical threshold was set at $|Z| > 1.96$ ($P < 0.05$) and cluster size $>1,404$ mm^3 (search volume: 1,575,720 mm^3), which corresponded to a corrected $P < 0.05$.

ALFF Analysis With GM Volume as Covariates

Recent studies of fMRI have suggested that functional results could potentially be influenced by structural differences among groups [He et al., 2007; Oakes et al., 2007]. To explore the possible effect, in this study, we performed a voxel-based morphometry (VBM) analysis for structural images. Briefly, GM intensity maps in the MNI space were obtained by the unified segmentation algorithm [Ashburner and Friston, 2005] as described in the previous Data Preprocessing section. As pointed out by Ashburner and Friston [2005], unified segmentation could solve the circularity problem of registration and tissue classification in optimized VBM [Good et al., 2001]. After spatially smoothed with a 10 mm full width at half maximum Gaussian kernel, one-way ANOVA was performed on the smoothed GM intensity maps across the three groups. The statistical threshold was set at $|Z| > 1.96$ ($P < 0.05$) and cluster size $>1,404$ mm^3 (search volume: 1,575,720 mm^3), which corresponded to a corrected $P < 0.05$. Furthermore, we reanalyzed the relative ALFF results (i.e., ANCOVA, two-sample *t*-tests and correlation analysis) by taking voxel-wise gray matter volume as covariates [Oakes et al., 2007], which was done by using REST-Statistical Analysis (written by Chaogan Yan, www.restfmri.net). The statistical threshold was also set at $|Z| > 1.96$ ($P < 0.05$) and

cluster size $>1,404$ mm^3 (search volume: 1,575,720 mm^3), which corresponded to a corrected $P < 0.05$.

RESULTS

Within-Group ALFF Maps

Figure 1 shows the ALFF maps of healthy elderly, AD, and MCI groups. Visual inspection indicated that the PCC and adjacent PCu had the highest ALFF values in all groups but exhibited different strengths (ALFF$_{AD}$ < ALFF$_{MCI}$ < ALFF$_{Healthy\ elderly}$). Additionally, we also noted that several other brain regions such as the MPFC and inferior parietal lobe (IPL) also exhibited high ALFF values. The ALFF patterns were highly similar to those of the human default-mode network demonstrated in previous studies [Greicius et al., 2003; Raichle et al., 2001]. Additionally, we also observed high ALFF in several other brain regions such as the occipital areas, pre and postcentral gyri. Here these within-group maps were merely for visualizing ALFF.

Group Differences in ALFF

Figure 2A shows the one-way ANOVA analysis of the ALFF values among the three groups. Significant group differences in ALFF were observed in frontal regions, including the MPFC/orbitofrontal gyrus (OFG), supplemental motor area (SMA), superior frontal gyrus (SFG), and middle frontal gyrus (MFG), in addition to temporal regions such as the inferior temporal gyrus (ITG), superior temporal gyrus (STG), fusiform gyrus (FG), parahippocampus (PHG), and hippocampus (Hip), as well as parietal regions such as the PCC/PCu, IPL, paracentral lobule (PCL), and postcentral gyrus (PoCG). There was little difference in the occipital lobes among the groups except for a small cluster of inferior occipital gyrus (IOG). Additionally, differences were also found in several subcortical regions such as the lentiform nucleus (LN) and anterior lobe of the cerebellum (ALC). Of note, the most significant differences appeared in the PCC/PCu. See Table II for a detailed list of the regions.

Figure 3A shows ALFF differences between AD patients and healthy elderly. The most significant ALFF decreases in the AD patients were found in the PCC/PCu, while decreases were also seen in the left OFG, left LN, and right ALC. Significant ALFF increases in AD were observed in the bilateral PHG/Hip, bilateral SMA, bilateral SFG, left FG, left ITG/STG and left PoCG. See Table III for the list of these regions.

Figure 4A shows ALFF differences between the MCI patients and healthy elderly. Interestingly, the changing ALFF patterns in MCI (Fig. 4A and Table IV) were very similar to those in AD patients as described above (Fig. 3A and Table III). That is, significant decreases in ALFF were mainly located at the bilateral PCC/PCu, bilateral SFG, left MFG, left LN, and left IPL. In addition, increases in ALFF were in the bilateral SMA, bilateral PCL, bilateral SFG, left PoCG, left FG, right IOG, and right ITG.
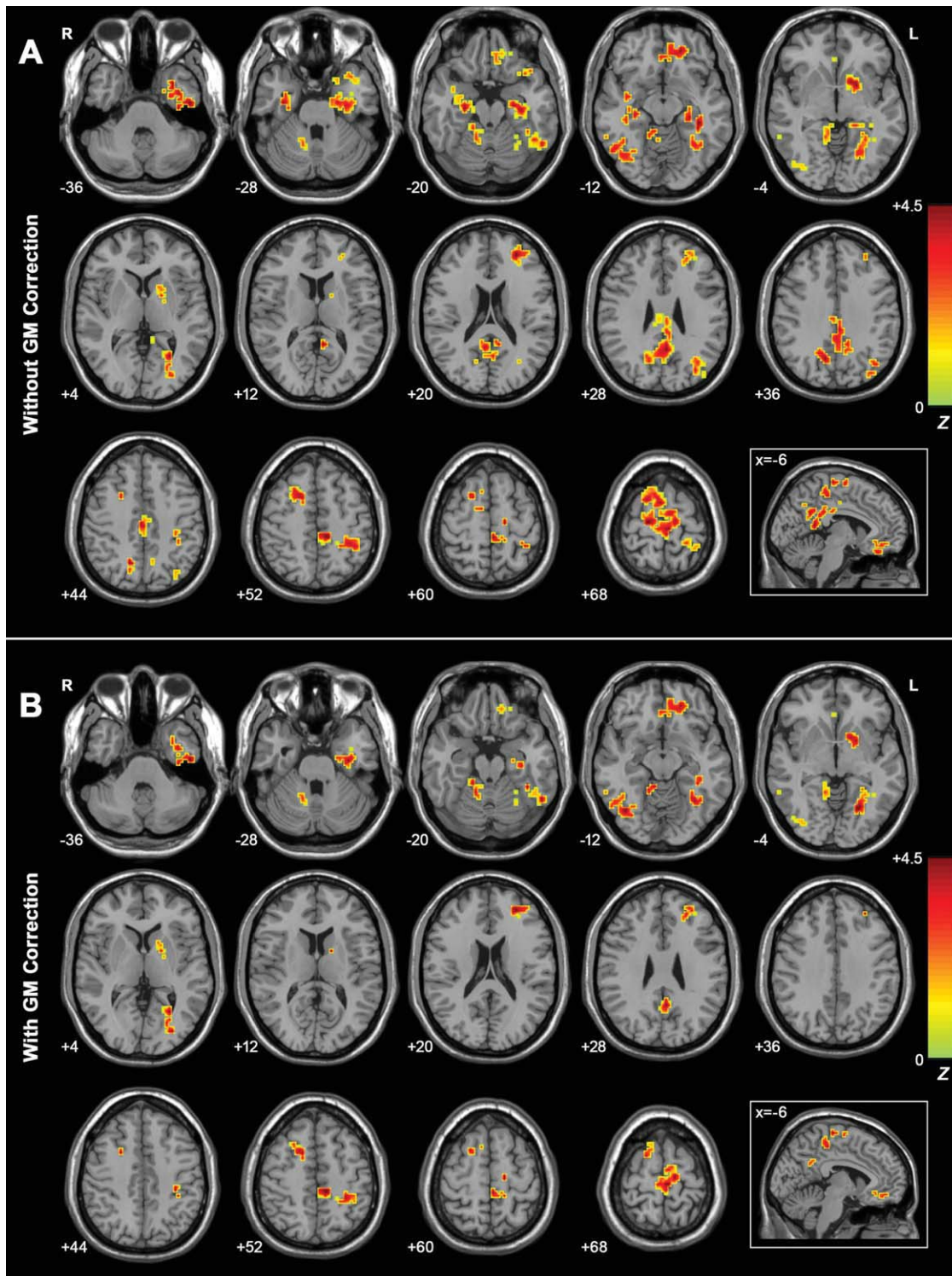
Figure 2.

A: Z-statistical maps among the AD, MCI, and healthy elderly (without GM correction). There were significant ALFF differences among the three groups in the bilateral PCC/PCu, bilateral PHG, bilateral Hip, bilateral ITG, bilateral SFG, bilateral SMA, left IPL, left LN, left FG, left STG, left PCL, left MFG, left MPFC, left OFG, left PoCG, right ALC, and right IOG. For the details of the regions, see Table II. **B**: Z-statistical maps among the AD, MCI and healthy elderly (with GM correction). There were significant ALFF differences among the three groups in the bilateral SFG, bilateral SMA, bilateral ITG, left PHG, left Hip, left STG, left FG, left PCL, left LN, left PoCG, left MFG, left MPFC, left OFG, right ALC, and right IOG. Additionally, we also found that there was a cluster in the PCC/PCu that survived the height but not the extent threshold. For the details of the regions, see Table II. The statistical threshold was set at $|Z| > 1.96$ ($P < 0.05$) and cluster size $>1,404$ mm^3, which corresponded to a corrected $P < 0.05$. Of note, we showed the ANCOVA results within a mask showing significant group differences in the ANOVA analysis (Fig. 2A). R, right; L, left. [Color figure can be viewed in the online issue, which is available at wileyonlinelibrary.com.]

TABLE II. Regions showing ALFF differences among the AD, MCI patients, and healthy controls (without and with GM correction)

Brain regions	BA	Vol (mm³)	MNI coordinates (mm)			Maximum Z
			x	y	z	
Without GM correction						
PCC/PCu	23/31/7	8,883	12	−63	33	7.92
Left PHG/Hip/STG	35/28/22	7,398	−33	−21	−24	7.54
Left LN	N/A	1,701	−21	6	−6	6.88
Left FG/ITG	37/36/20	4,104	−27	−60	6	6.86
Right PHG/Hip	35/36	2,538	36	−12	−27	6.75
Left IPL	40	1,620	−33	−75	30	6.54
Left PCL	5	4,779	−9	−30	54	6.24
Left MFG/MPFC/OFG	10/11	2,133	−18	42	−12	5.87
Left SFG/MFG	10/11	1,890	−27	45	18	5.80
SFG/SMA	5/6	3,591	3	3	69	5.65
Right ALC	N/A	1,890	6	−36	−6	5.52
Left PoCG	40	1,944	−39	−42	51	5.51
Right IOG/ITG	19/37	2,160	39	−69	−9	4.99
With GM correction						
Left PHG/Hip/STG	35/28/22	2,484	−33	−21	−24	7.51
Left FG/ITG	37/36/20	3,537	−27	−60	6	6.83
Left PCL	5	3,267	−9	−30	54	6.41
Right IOG/ITG	19/37	1,998	39	−66	−12	6.34
Left LN	N/A	1,296	−21	6	−6	6.12
Left PoCG	40	864	−33	−27	42	6.03
Right ALC	N/A	1,620	9	−42	−12	6.01
Left MFG/MPFC/OFG	10/11	1,566	−18	42	−12	5.97
PCC/PCu[a]	23/31/7	837	−3	−51	30	5.78
SFG/SMA	5/6	1,593	15	9	51	5.57
Left SFG/MFG	10/11	1,512	−27	39	15	5.18

x, y, z, coordinates of primary peak locations in the MNI space; Z, statistical value of peak voxel showing ALFF differences among the three groups. ALC, anterior lobe of cerebellum; BA, Brodmann's area; FG, fusiform gyrus; Hip, hippocampus; IOG, inferior occipital gyrus; IPL, inferior parietal lobule; ITG, inferior temporal gyrus; LN, lentiform nucleus; MFG, middle frontal gyrus; MPFC, medial prefrontal cortex; N/A, not applicable; OFG, orbitofrontal gryus; PCC/PCu, posterior cingulate cortex/precuneus; PCL, paracentral lobule; PHG, parahippocampa gyrus; PoCG, postcentral gyrus; SFG, superior frontal gyrus; SMA, supplementary motor area; STG, superior temporal gyrus. $P < 0.05$, corrected for multiple comparisons.
[a]The PCC survived the height but not the extent threshold.

However, we also noted that there were some discrepancies in the changing ALFF patterns in MCI. For instance, The ALFF values showed significant differences in the bilateral PHG/Hip and left OFG between the AD patients and healthy elderly, but were unchanged between the MCI patients and healthy elderly.

Figure 5A shows a direct comparison of the ALFF values between the AD and MCI patients. Compared with the MCI patients, the AD patients showed significantly decreased ALFF in the left MPFC/OFG and increased ALFF in the right SFG, left ITG, and left STG. (Fig. 5A, Table V).

PCC ALFF Analyses

As shown above, the PCC is the region with the most significant ALFF differences among the three groups, which raises a possibility that the ALFF values for the PCC might serve as markers to differentiate the AD/MCI patients from healthy controls. To explore the possibility, we first calculated the mean ALFF value of each subject within a PCC mask (Fig. 6A), where the mask was composed of the bilateral posterior cingulate gyri in the automated anatomical labeling (AAL) template [Tzourio-Mazoyer et al., 2002]. Subsequently, the group differences were measured using ANOVA. As expected, the ALFF values of PCC for all groups had a pattern of $ALFF_{AD} < ALFF_{MCI} < ALFF_{healthy\ elderly}$ (Fig. 6B,C) ($F = 3.18$, $P = 0.05$), but significant differences only existed between the AD patients and healthy elderly ($t = −3.87$, $P = 0.0004$). Furthermore, we plotted receiver operating characteristic curves (ROC) to explore whether the PCC ALFF values could differentiate the patients from the healthy controls. Figure 6D shows the sensitivity and specificity of the
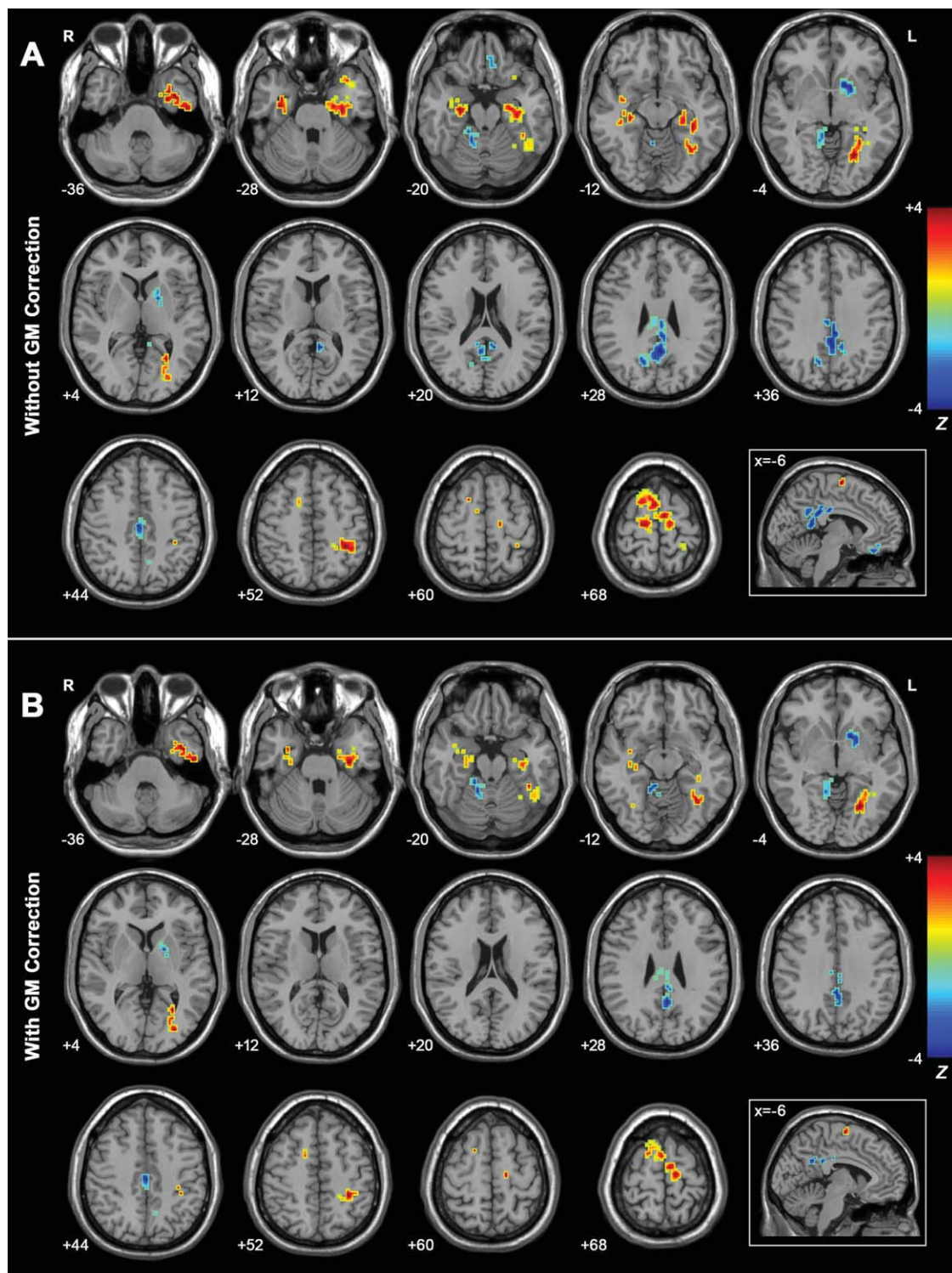
Figure 3.

A: Z-statistical difference maps between the AD patients and healthy eldely (without GM correction). The AD patients showed significantly decreased ALFF in the bilateral PCC/PCu, left LN, left OFG, and right ALC, and increased ALFF in the bilateral PHG, bilateral Hip, bilateral SFG, bilateral SMA, left FG, left PoCG, left ITG, and left STG. For the details of the regions, see Table III. **B**: Z-statistical difference maps between the AD patients and healthy elderly (with GM correction). The AD patients showed significantly decreased ALFF in the bilateral PCC/PCu, left LN, and right ALC, and increased ALFF in the bilateral PHG, bilateral Hip, bilateral SFG, bilateral SMA, left FG, left PoCG, left ITG, and left STG. For the details of the regions, see Table III. The statistical threshold was set at $|Z| > 1.96$ ($P < 0.05$) and cluster size $>1,404$ mm^3, which corresponded to a corrected $P < 0.05$. Of note, we showed the two-sample t-tests results within a mask showing significant group differences in the ANOVA analysis (Fig. 2A). R, right; L, left. [Color figure can be viewed in the online issue, which is available at wileyonlinelibrary.com.]

TABLE III. Regions showing ALFF differences between the AD patients and healthy controls (without and with GM correction)

Brain regions	BA	Vol (mm³)	MNI coordinates (mm)			Maximum Z
			x	y	z	
Without GM correction						
PCC/PCu	23/7/29	6,939	−3	−36	30	−4.24
Left LN	N/A	1,593	−21	6	−6	−3.65
Right ALC	N/A	459	15	−48	−21	−3.52
Left OFG	11	351	−6	33	−21	−2.77
Left PHG/Hip	35/36/28	3,078	−30	−18	−24	4.34
Right SFG/SMA	6	2,079	3	3	69	4.01
Left FG	37	3,321	−27	−57	0	3.95
Left SFG/SMA	6	1,053	−6	−9	66	3.81
Right PHG/Hip	35/28	1,728	30	−18	−27	3.79
Left PoCG	40	1,107	−30	−33	48	3.55
Left ITG/STG	20/22	2,835	−39	−3	−42	3.40
With GM correction						
PCC/PCu	23/7/29	1,161	−3	−51	30	−3.54
Left LN	N/A	1,161	−18	3	6	−3.43
Right ALC	N/A	1,296	15	−48	−18	−3.60
Left PHG/Hip	35/36/28	1,134	−30	−18	−24	4.20
Left FG	37	3,240	−33	−57	−15	4.09
Left PoCG	40	621	−30	−33	48	3.82
SFG/SMA	6	1,053	3	3	69	3.51
Left ITG/STG	20/22	1,350	−39	−3	−39	3.48
Right PHG/Hip	35/28	783	33	−3	−27	3.15

x, y, z, coordinates of primary peak locations in the MNI space; Z statistical value of peak voxel showing ALFF differences between the AD subjects and healthy elders (negative values: AD < NC; positive values: AD > NC). ALC, anterior lobe of cerebellum; BA, Brodmann's area; FG, fusiform gyrus; Hip, hippocampus; ITG, inferior temporal gyrus; LN, lentiform nucleus; N/A, not applicable; OFG, orbitofrontal gryus; PCC/PCu, posterior cingulate cortex/precuneus; PHG, parahippocampal gyrus; PoCG, postcentral gyrus; SFG, superior frontal gyrus; SMA, supplementary motor area; STG, superior temporal gyrus. $P < 0.05$, corrected for multiple comparisons.

ALFF of PCC for the AD and control subjects. The cut-off point of the ALFF value for sensitivity and specificity evaluations was 1.02. Using this cut-off value, the ALFF of the PCC correctly classified 16 of 22 controls and 13 of 16 AD subjects, yielding a sensitivity of 81% and specificity of 73%. The area under the curve for the ROC was 0.82 (95% confidence intervals from 0.67 to 0.96), thereby indicating that the PCC ALFF values could be used as markers for the diagnosis of early AD. However, further ROC analysis revealed that the PCC ALFF values were not able to differentiate the MCI subjects from the AD or healthy subjects (data not shown).

Correlations Between the ALFF and MMSE

Figure 7A shows the correlation maps between the ALFF and MMSE scores in the combined AD and MCI groups. There were significant negative correlations found in the bilateral PHG, left ITG, and right SFG and significant positive correlations in the Left MPFC/OFG and left PCL (Fig. 7A, Table VI). Additionally, we also found that there were two clusters in the left PCC and right PCu that survived the height but not the extent threshold (Fig. 7A, Table VI).

ALFF Analysis With GM Volume as Covariates

We performed a VBM analysis to reveal the GM volume differences among the three groups. The results showed most significant differences in the frontal, temporal, and parietal regions (see Fig. 8). While taking regional GM volume as covariates, we found that the results of ALFF (Figs. 2B, 3B, 4B, 5B, 7B and 7C. For details, see Table II–VI) were approximately consistent with those without GM correction. However, we also noted that some results were partly influenced after GM correction. For example, there was a 8,883-mm³ cluster in the PCC/PCu showing significantly group differences in ALFF (Fig. 2A) but the cluster decreased to 837 mm³ after the GM correction (Fig. 2B).

DISCUSSION

The current study investigated the AD- and MCI-related changes in the intrinsic or spontaneous brain activity by
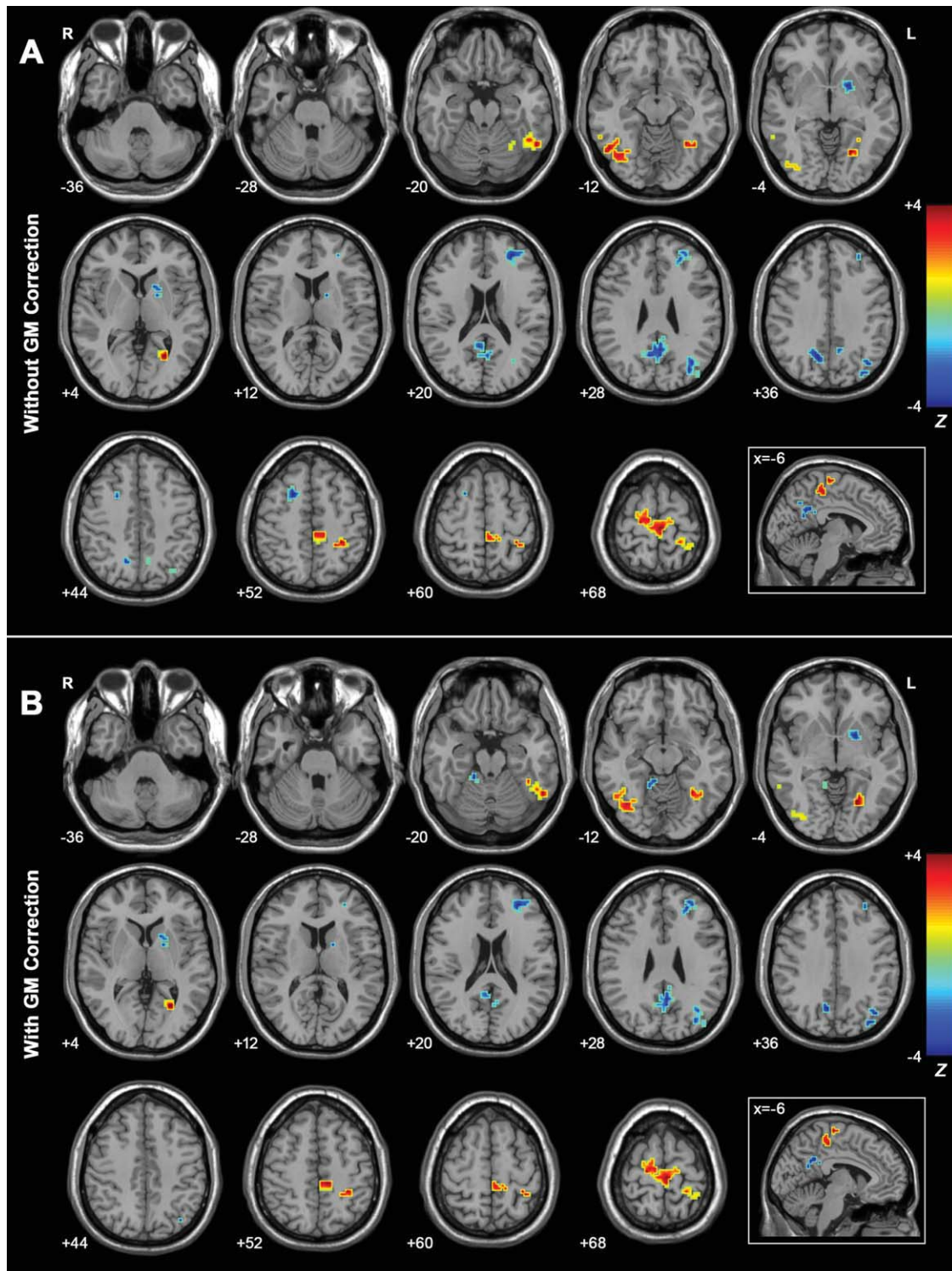
Figure 4.

A: Z-statistical difference maps between the MCI patients and healthy elderly (without GM correction). The MCI patients showed significantly decreased ALFF in the bilateral PCC/PCu, bilateral SFG, left IPL, left MFG, and left LN, and increased ALFF in the bilateral SMA, bilateral PCL, left PoCG, left FG, right IOG, and right ITG. For the details of the regions, see Table IV. **B**: Z-statistical difference maps between the MCI patients and healthy elderly (with GM correction). The MCI patients showed significantly decreased ALFF in the bilateral PCC/PCu, left MFG, left SFG, left IPL, left LN, right ALC and increased ALFF in the bilateral SMA, bilateral PCL, left FG, left PoCG, right IOG, and right ITG. For the details of the regions, see Table IV. The statistical threshold was set at $|Z| > 1.96$ ($P < 0.05$) and cluster size $>1,404$ mm^3, which corresponded to a corrected $P < 0.05$. Of note, we showed the two-sample t-tests results within a mask showing significant group differences in the ANOVA analysis (Fig. 2A). R, right; L, left. [Color figure can be viewed in the online issue, which is available at wileyonlinelibrary.com.]

TABLE IV. Regions showing ALFF differences between the MCI patients and healthy controls (without and with GM correction)

Brain regions	BA	Vol (mm³)	MNI coordinates (mm)			Maximum Z
			x	y	z	
Without GM correction						
Left IPL	39/40	1,485	−36	−75	30	−4.24
Left MFG/SFG	10/6	1,782	−27	39	15	−3.76
PCC/PCu	31/23/7	4,023	12	−60	33	−3.76
Right SFG	6	756	21	12	51	−3.36
Left LN	N/A	891	−18	6	−3	−3.09
PCL/SFG/SMA	5/6	3,537	−3	−30	66	3.58
Left PoCG	40	1,107	−30	−39	51	3.52
Left FG	37	1,458	−54	−54	−18	3.44
Right IOG/ITG	19/37	2,133	51	−60	−12	3.10
With GM correction						
Left MFG/SFG	10	1,620	−27	39	15	−3.78
Left IPL	39/40	1,161	−36	−75	30	−3.70
Right ALC	30	540	9	−42	−12	−3.36
PCC/PCu	31/23/7	1,755	12	−60	33	−3.14
Left LN	N/A	864	−18	6	−3	−3.04
Left FG	37	1,215	−30	−54	−12	4.08
PCL/SFG/SMA	5/6	3,456	−9	−30	54	3.82
Right IOG/ITG	19/37	1,971	39	−69	−9	3.76
Left PoCG	40	1,026	−30	−39	51	3.51

x, y, z, coordinates of primary peak locations in the MNI space; Z, statistical value of peak voxel showing ALFF differences between the MCI subjects and healthy elders (negative values: MCI < NC; positive values: MCI > NC). ALC, anterior lobe of cerebellum; BA, Brodmann's area; FG, fusiform gyrus; IOG, inferior occipital gyrus; IPL, inferior parietal lobule; ITG, inferior temporal gyrus; LN, lentiform nucleus; MFG, middle frontal gyrus; N/A, not applicable; PCC/PCu, posterior cingulate cortex/precuneus; PCL, paracentral Lobule; PoCG, postcentral gyrus; SFG, superior frontal gyrus; SFG, superior frontal gyrus; SMA, supplementary motor area. $P < 0.05$, corrected for multiple comparisons.

measuring the ALFF values of resting-state fMRI signals. We found that there were widespread differences in ALFF values among the AD, MCI patients, and healthy elderly throughout the various brain regions of the frontal, temporal, and parietal lobes, as well as subcortical areas. Of these, decreased ALFF values were observed in both AD and MCI patients in the medial parietal regions (PCC and PCu) and subcortical regions (LN). In contrast, increased ALFF values were mainly observed in the lateral temporal cortex (ITG and FG), lateral parietal cortex (PoCG) and superior frontal cortex (SFG/SMA). Moreover, several brain regions also showed significant ALFF differences between the AD and MCI patients, which were mainly in the MPFC/OFG, SFG and ITG. Specifically, the most significant ALFF difference among the three groups appeared in the PCC, which followed a general pattern of $ALFF_{AD} < ALFF_{MCI} < ALFF_{healthy\ elderly}$. Further analysis revealed that the ALFF value for the PCC can be applied to differentiate AD patients from healthy controls with a high sensitivity and specificity. We also found that many brain regions with group ALFF differences showed significant correlations with the performance of cognitive function measured with MMSE. Finally, we showed that our results of ALFF still remain significant after statistically control-ling for the regional atrophy. Our results suggest that the ALFF measurement of intrinsic or spontaneous brain activity could be useful to characterize the physiology of AD and MCI.

The Nature of ALFF

Recent resting fMRI studies have suggested that the ALFF of BOLD signals are physiologically meaningful. However, the exact biological mechanisms behind ALFF remain unclear to date. Nonetheless, several researchers have indicated that the ALFF likely reflects regional spontaneous neuronal activity. For instance, Biswal et al. [1995] found that the root mean square of the LFF in the white matter was reduced by about 60% relative to the gray matter. By simultaneously monitoring the local field potential and task-induced BOLD signal in anesthetized monkeys, Logothetis et al. [2001] found that the task-induced BOLD signal closely related to the local field potential. Shmuel and Leopold [2008] found significant correlations between the LFF and gamma band activity with simultaneous electrophysiological recordings in monkeys. Lu et al. [2007] found that the LFF was greatly associated with the delta band of electrophysiological recordings in rats. Goldman
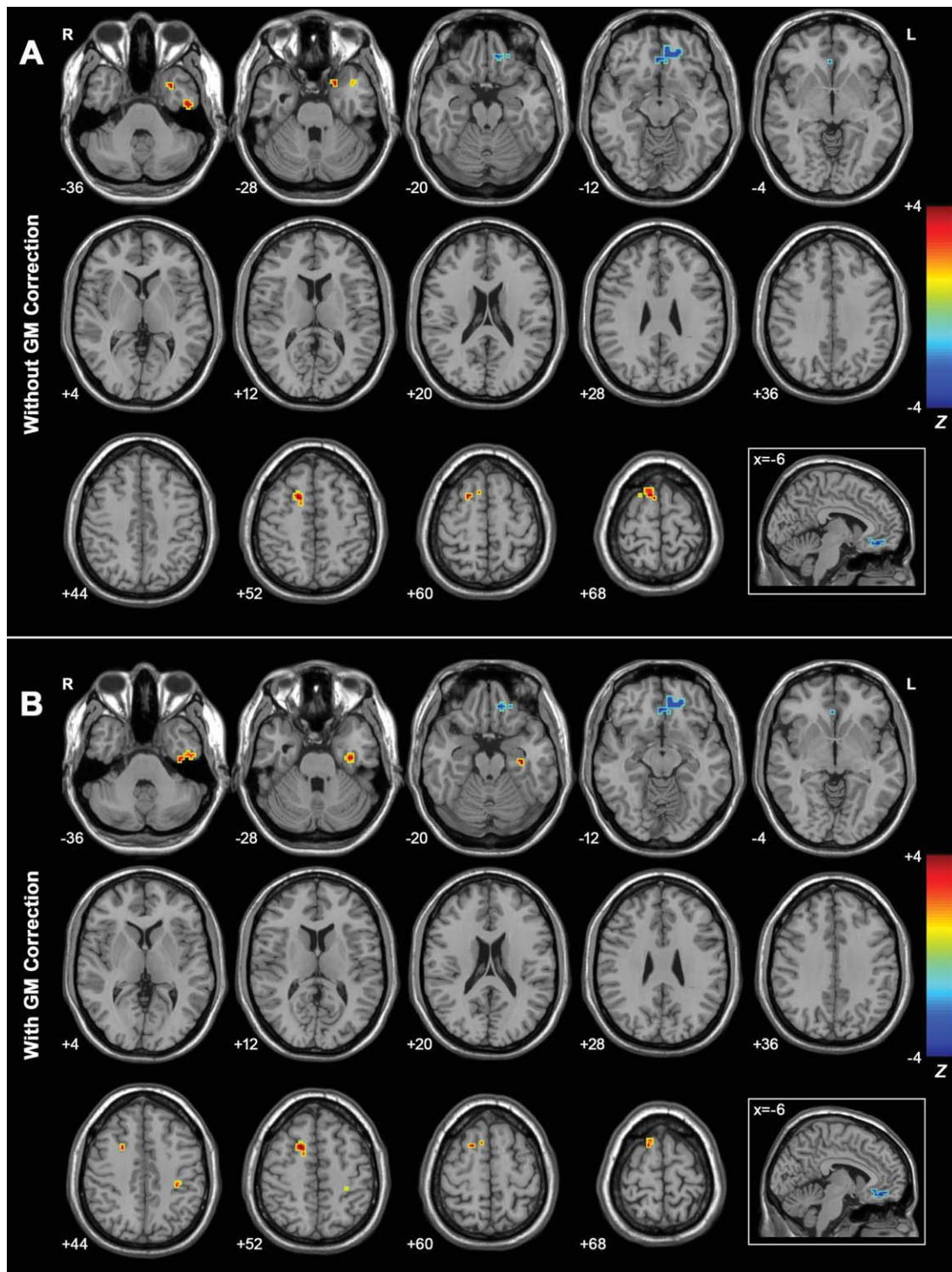
Figure 5.

A: *Z*-statistical difference maps between the AD and MCI patients (without GM correction). The AD patients showed significantly decreased ALFF in the left MPFC/OFG and increased ALFF in the right SFG, left ITG, and left STG. For the details of the regions, see Table V. **B**: *Z*-statistical difference maps between the AD and MCI patients (with GM correction). The AD patients showed significantly decreased ALFF in the left MPFC/OFG and increased ALFF in the right SFG and left ITG. For the details of the regions, see Table V. The statistical threshold was set at $|Z| > 1.96$ ($P < 0.05$) and cluster size $> 1,404$ mm^3, which corresponded to a corrected $P < 0.05$. Of note, we showed the two-sample *t*-tests results within a mask showing significant group differences in the ANOVA analysis (Fig. 2A). R, right; L, left. [Color figure can be viewed in the online issue, which is available at wileyonlinelibrary.com.]

TABLE V. Regions showing ALFF differences between the AD and MCI patients (without and with GM correction)

Brain regions	BA	Vol (mm^3)	MNI coordinates (mm)			Maximum Z
			x	y	z	
Without GM correction						
Left MPFC/OFG	11	1,404	−9	39	−18	−2.37
Right SFG	6	837	18	9	54	2.39
Right SFG	6	459	12	18	66	2.04
Left ITG	20	378	−51	−12	−39	1.83
Left STG	38	783	−39	12	−33	1.82
With GM correction						
Left MPFC/OFG	11	1,458	−9	39	−18	−2.42
Left ITG	20	1,026	−36	−15	−42	2.39
Right SFG	6	891	18	9	54	2.23
Right SFG	6	270	12	18	66	1.75

x, y, z, coordinates of primary peak locations in the MNI space; Z, statistical value of peak voxel showing ALFF differences between the AD and MCI subjects (negative values: AD < MCI; positive values: AD > MCI). BA, Brodmann's area; ITG, inferior temporal gyrus; MPFC, medial prefrontal cortex; OFG, orbit frontal gyrus; SFG, superior frontal gyrus; STG, superior temporal gyrus. $P <$ 0.05, corrected for multiple comparisons.

et al. [2002] and Moosmann et al. [2003] also found the LFF in the visual cortex was closely associated with alpha band power in humans. These converging lines of evidence suggest that regional BOLD LFF signals may reflect spontaneous neural activity. By measuring the amplitude of the spontaneous activities (ALFF), several researchers have shown altered baseline brain activity in children with attention deficit hyperactivity disorder [Zang et al., 2007] and trauma survivors shortly after traumatic events [Lui et al., 2009]. Two recent resting fMRI studies also utilized ALFF to investigate the brain's spontaneous activity under eyes-open and eyes-closed conditions, and found that the activities within the visual cortex and default-mode regions were significantly different between the two conditions [Yan et al., 2009; Yang et al., 2007]. These recent studies indicate that the ALFF is physiologically meaningful for measuring intrinsic or spontaneous neuronal activity of the brain.

Decreased ALFF in AD and MCI

We found that both the AD and MCI patients showed decreased ALFF in several brain regions including the PCC, PCu, and LN compared with the healthy controls (Figs. 3A and 4A). Of these regions, the PCC showed the most significant ALFF differences among the three groups. Recent studies have suggested that the PCC is mainly involved in episodic memory processing [Buckner et al., 2008; Gusnard et al., 2001) and it is a critical node in human brain structural and functional networks [Buckner et al., 2009; Gong et al., 2009; Greicius et al., 2003; Hag-

mann et al., 2008]. Many neuroimaging studies have also consistently demonstrated that this region had structural and functional abnormalities in both AD and MCI patients, such as cortical thinning [Dickerson et al., 2009; He et al., 2008; Lerch et al., 2005; Singh et al., 2006], metabolic pathologies [de Leon et al., 2001; Salmon et al., 2000; Volkow et al., 2002], and disruptions in spontaneous or intrinsic brain activity [Bai et al., 2008; Buckner et al., 2009; Greicius et al., 2004; He et al., 2007; Sorg et al., 2007; Wang et al., 2006; Zhang et al., 2009]. Thus, our finding of decreased ALFF in AD and MCI subjects was in accordance with these previous studies. Furthermore, we observed that the ALFF activity for the PCC exhibited a general pattern of ALFF$_{AD}$ < ALFF$_{MCI}$ < ALFF$_{healthy\ elderly}$, which was also compatible with the notion that MCI is a transition stage between healthy elderly and AD. In this study, we noticed that there were positive correlations between the ALFF of the PCC and MMSE scores, thereby indicating that the changes in ALFF for this region were associated with cognitive performance in these patients. Specifically, while taking the ALFF values of the PCC as an index, we were able to differentiate AD patients from healthy elderly controls (with a high specificity of 73% and a high sensitivity of 81%), implying the PCC can serve as an imaging biomarker for the early diagnosis of AD.

Besides the PCC region, we also found decreased ALFF activity in the PCu of the AD and MCI patients. The PCC and adjacent PCu (i.e., medial parietal lobe regions) were often observed to show parallel structural and functional abnormalities in previous brain imaging studies of AD and MCI subjects [Buckner et al., 2005, 2009; Dickerson et al., 2009; He et al., 2008; Lustig et al., 2003; Salmon et al., 2000; Volkow et al., 2002]. Thus, our results provide further support for abnormal PCu activity in AD and MCI patients. Additionally, the LN was also found to have decreased ALFF activity in the AD and MCI patients. Although the region has been less investigated in resting fMRI studies, their structural and functional abnormalities have been demonstrated in several previous AD/MCI studies [Baron et al., 2001; Bokde et al., 2006].

Increased ALFF in AD and MCI

We also found that both AD and MCI patients showed increased ALFF in the FG, SFG, SMA, and PoCG (Figs. 3A and 4A). The FG is mainly involved in the processing of memory [Kohler et al., 1998] and facial stimuli [Allison et al., 1994; Haxby et al., 1996, 2001; Kanwisher et al., 1997]. Functional imaging studies have indicated that this region usually shows increased activity in AD/MCI patients during cognitive tasks and the resting state. For example, Prvulovic et al. [2002] observed that AD patients had increased functional activation in the FG during visuospatial processing. Bokde et al. [2006] found that MCI patients showed widespread changes in functional connectivity of FG during performance of a face-matching task. Recently, He et al. [2007] demonstrated that the FG
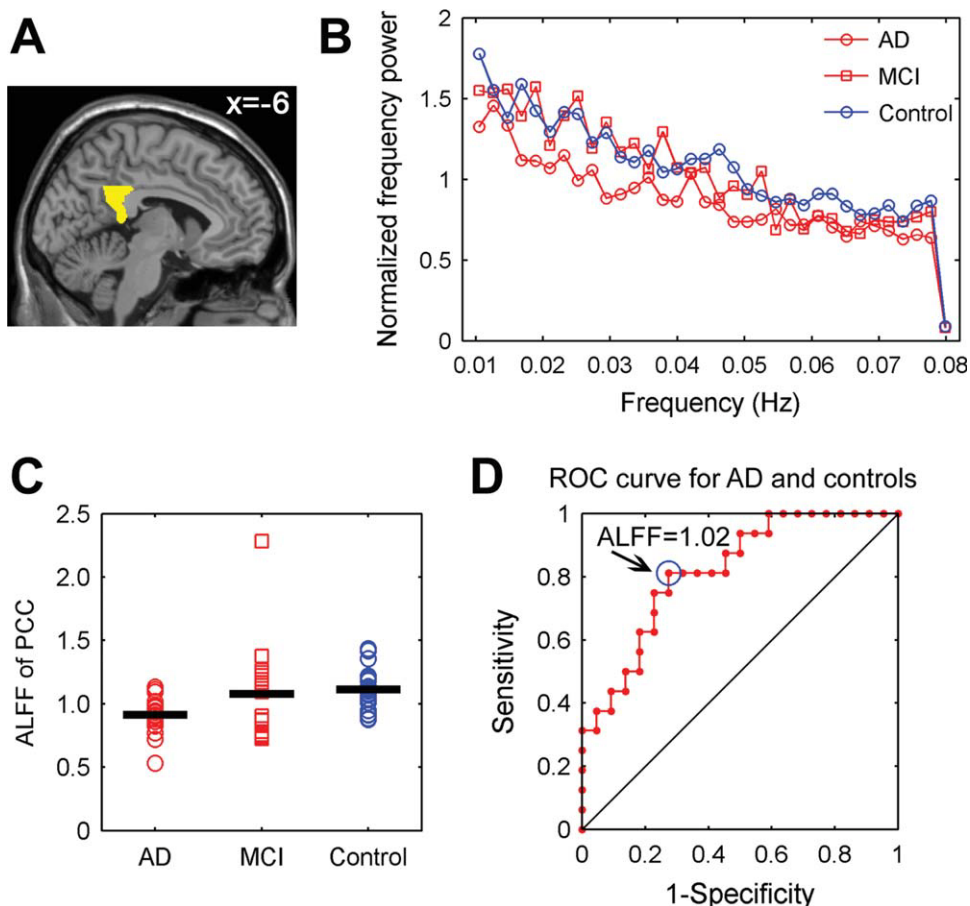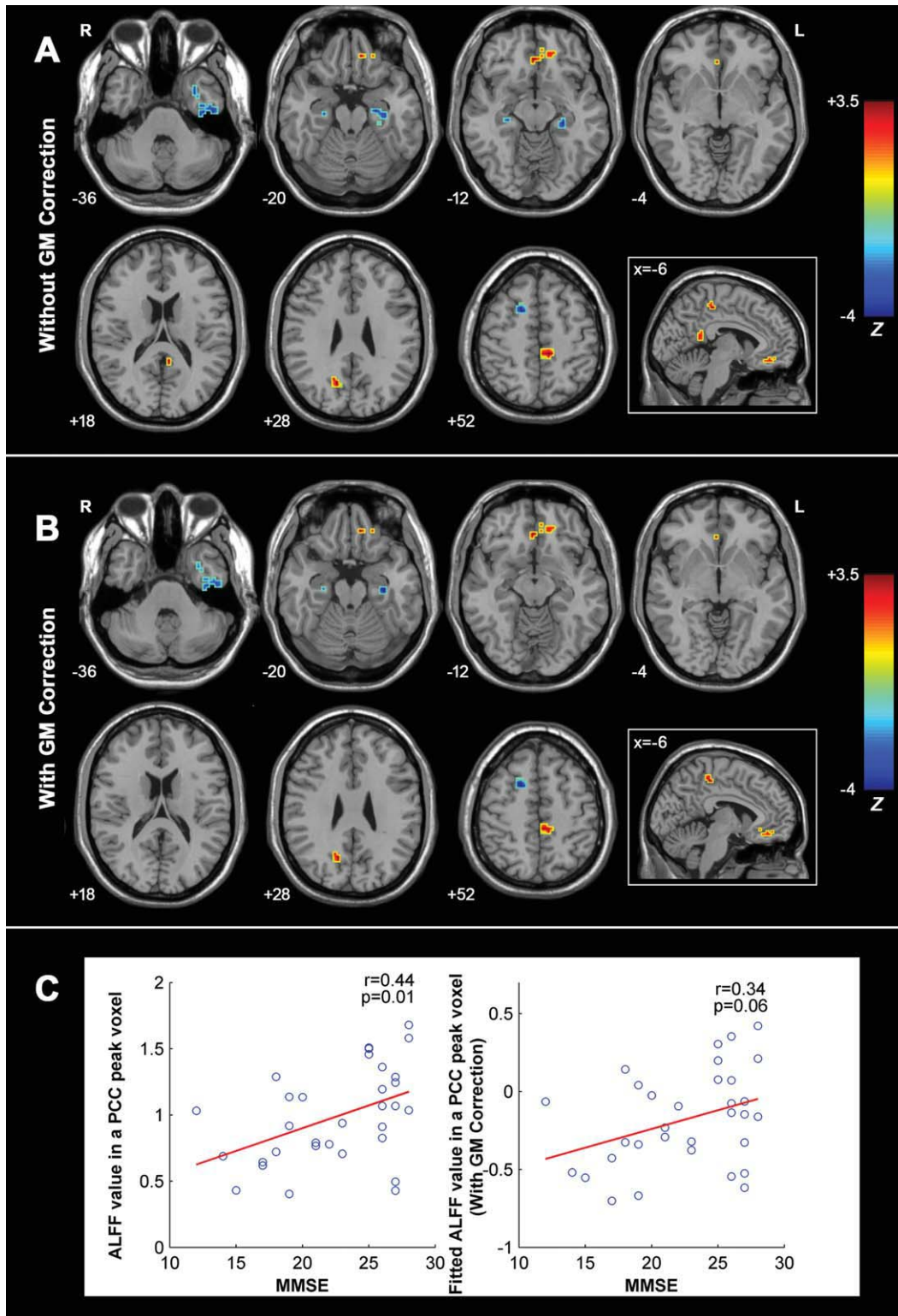
Figure 6.

The ALFF of PCC. **A**: The PCC mask extracted from the AAL template. **B**: Averaged normalized frequency power of the PCC in the AD, MCI, and healthy elderly groups. Visual examination indicated that the AD patients exhibited the lowest frequency power of PCC compared with the MCI patients and healthy controls. **C**: A scatter plot showing individual PCC ALFF in the AD, MCI, and healthy elderly groups. The group means were different among the three groups and showed a trend of $ALFF_{AD}$ < $ALFF_{MCI}$ < $ALFF_{healthy\ elderly}$. There were significant differences between the AD patients and healthy elderly ($t = -3.87$, $P = 0.0004$) but not between the AD and MCI patients ($t = -1.57$, $P = 0.13$), and between the MCI patients and healthy elderly ($t = -0.37$, $P = 0.71$). Of note, there was an outlier in the data of MCI patients according to the Dixon's test ($r = 0.66$, $P < 0.005$). While excluding the data of this patient, there were still significant differences between the AD patients and healthy elderly ($t = -3.87$, $P = 0.0004$) but not between the AD and MCI patients ($t = -1.21$, $P = 0.24$), and between the MCI patients and healthy elderly ($t = -1.78$, $P = 0.08$). **D**: A receiver operating characteristic (ROC) curve for AD and healthy controls. The circle indicates a cutoff point of 1.02. Using this cut-off value, 13 of 16 AD subjects and 16 of 22 elderly subjects were correctly classified, yielding a sensitivity of 81% and a specificity of 73%. The area under the curve for the ROC was 0.82 (95% confidence intervals 0.67 to 0.96). Notably, the PCC ALFF index was not able to well discriminate the MCI subjects from either AD subjects or healthy controls (data not shown). [Color figure can be viewed in the online issue, which is available at wileyonlinelibrary.com.]

had increased functional homogeneity of intrinsic brain activity in AD patients using resting fMRI. Thus, our results demonstrating increased ALFF in AD and MCI patients were compatible with these previous studies. Likewise, the findings of AD- and MCI-related ALFF increases in the frontal regions (SFG and SMA) were also in accordance with previous studies. For example, several groups have reported increased prefrontal activity during some cogni-

tive tasks in AD patients compared with healthy elders [Backman et al., 1999; Becker et al., 1996; Gould et al., 2006; Grady et al., 2003; Saykin et al., 1999]. AD-related increases in the functional connectivity of prefrontal regions have also been reported in several studies [Horwitz et al., 1995; Wang et al., 2006]. In a recent fMRI study, Yetkin et al. [2006] found that both AD and MCI patients had more functional activation in the SFG and FG during

Figure 7.

A: Correlation maps of MMSE score and ALFF for the AD and MCI patients ($n = 32$) (without GM correction). Significant negative correlations were found in the bilateral PHG, left ITG, and right SFG, and positive correlations in the left MPFC/OFG and left PCL. Additionally, we also found that there were two clusters in the left PCC and right PCu that survived the height but not extent threshold. For the details of the regions, see Table VI. **B**: Correlation maps of MMSE score and ALFF for the AD and MCI patients ($n = 32$) (with GM correction). Significant negative correlations were found in the bilateral PHG, left ITG and right SFG, and positive correlations in the left MPFC and left PCL. We also observed that there was a cluster in the right PCu that survived the height but not extent threshold. For the details of the regions, see Table VI. The statistical threshold was set at $|Z| > 1.96$ ($P < 0.05$) and cluster size $> 1,404$ mm^3, which corresponded to a corrected $P < 0.05$. Of note, we showed the correlation results within a mask showing significant group differences in the ANOVA analysis. R, right; L, left. **C**: The scatter plots between ALFF of PCC and MMSE scores with and without GM correction. [Color figure can be viewed in the online issue, which is available at wileyonlinelibrary.com.]

TABLE VI. Regions showing significant correlations between ALFF and MMSE for the AD and MCI patients (without and with GM correction)

Brain regions	BA	Vol (mm³)	MNI coordinates (mm)			Maximum Z
			x	y	z	
Without GM correction						
Left PHG/ITG	20	1,917	−36	−15	−42	−4.84
Right PHG	20	270	36	−12	−27	−4.19
Right SFG	8	1,161	21	12	57	−3.26
Left PCL	5	702	−12	−33	51	3.48
Left MPFC/OFG	11	918	−9	39	−18	3.19
Right PCu[a]	31	351	15	−66	24	2.58
Left PCC[a]	29	189	−6	−48	15	2.52
With GM correction						
Left PHG/ITG	20	1,134	−36	−15	−42	−4.76
Left PHG/ITG	20/19	351	−33	−21	−24	−3.35
Right PHG	20	135	27	−15	−24	−3.21
Right SFG	8	1,026	21	12	57	−3.14
Left MPFC/OFG	11	702	−9	39	−18	3.21
Left PCL	5	540	−6	−33	51	3.07
Right PCu[b]	31	297	15	−66	24	2.54

x, y, z, coordinates of primary peak locations in the MNI space; Z, statistical value of peak voxel showing significant correlations between ALFF and MMSE score in the AD and MCI subjects. Negative Z values indicate negative correlations between ALFF and MMSE scores, vice versa. BA, Brodmann's area; ITG, inferior temporal gyrus; MPFC, medial prefrontal cortex; PCC, posterior cingulate cortex; PCL, paracentral lobule; PCu, precuneus; PHG, parahippocampa gyrus; SFG, superior frontal gyrus. $P < 0.05$, corrected for multiple comparisons.
[a]Two clusters in the PCC (243 mm³) and PCu (459 mm³) survived the height but not the extent threshold.
[b]The cluster in the PCu (378 mm³) survived the height but not the extent threshold.

a working memory task as compared with controls, which was consistent with our results. The increased functional activity or functional connectivity has been proposed as a compensatory reallocation or recruitment of cognitive resources in AD/MCI patients [Bokde et al., 2006; Grady et al., 2003; He et al., 2007; Prvulovic et al., 2002]. Our findings demonstrating the negative correlations between the ALFF values of the SFG and MMSE scores provide further support for this compensatory hypothesis.

ALFF Differences Between the AD and MCI Groups

ALFF differences were also found between the AD and MCI patients (Fig. 5A). Compared with the MCI patients, the AD patients showed decreased ALFF mainly in the MPFC/OFG. The regions are considered important components of human default-mode networks [Buckner et al., 2008; Greicius et al., 2003; Raichle et al., 2001) and have

been shown to exhibit AD- and MCI-related structural and functional abnormalities. Our finding of decreased ALFF in AD patients reflects a continuous breakdown of spontaneous brain activity during disease progression. In this study, we also observed that AD patients showed increased ALFF in several frontal and temporal regions (e.g., SFG, ITG, and STG) as compared with the MCI patients. These increases could be interpreted as compensatory reallocation or recruitment of cognitive resource (see the above section). It is worthy to note that a previous resting fMRI study showed increased functional connectivity between the right lateral prefrontal cortex and left hippocampus in AD patients [Wang et al., 2006]. The increased frontal activation/connectivity has been proposed as compensatory mechanisms in patients with AD. It should be noted that the analytic approach (ALFF) used in this study is very different from those applied in the previous studies. Based on these considerations, we speculate that the increases of ALFF in the AD patients could be biologically meaningful (e.g., reflect a compensatory recruitment), but it needs to be further confirmed in future studies.

ALFF Analysis with GM Correction

This study examined the ALFF changes in AD and MCI by using resting fMRI and whether the functional results could be influenced by regional GM atrophy. As we have known, AD and MCI are associated with widespread GM loss in many brain regions involving the frontal, temporal, and parietal regions [Baron et al., 2001; Buckner et al., 2005; Dickerson et al., 2009; He et al., 2008; Lerch et al., 2005). The GM atrophy may lead to artificial reduction in measured functional signals. While comparing functional differences among the AD, MCI patients, and controls, this issue could potentially be crucial due to individual or group differences in the degree of regional atrophy. Several recent fMRI studies have attempted to clarify the relationship between regional GM atrophy and BOLD signals during the performance of tasks [Johnson et al., 2000; Oakes et al., 2007; Prvulovic et al., 2002) and the resting-state [He et al., 2007]. Most of them found that the functional results still retained statistically significant but reduced significance after GM correction. In this study, after controlling for the regional atrophy, we found that the results of ALFF were partly influenced, but the patterns were approximately consistent with those without GM correction. It implies that our results of ALFF could reflect the changes in intrinsic brain functional activities in the patients.

Further Considerations

Notably, several issues need to be further addressed. First, in this investigation all participants were instructed to close their eyes during the resting-state scans. This
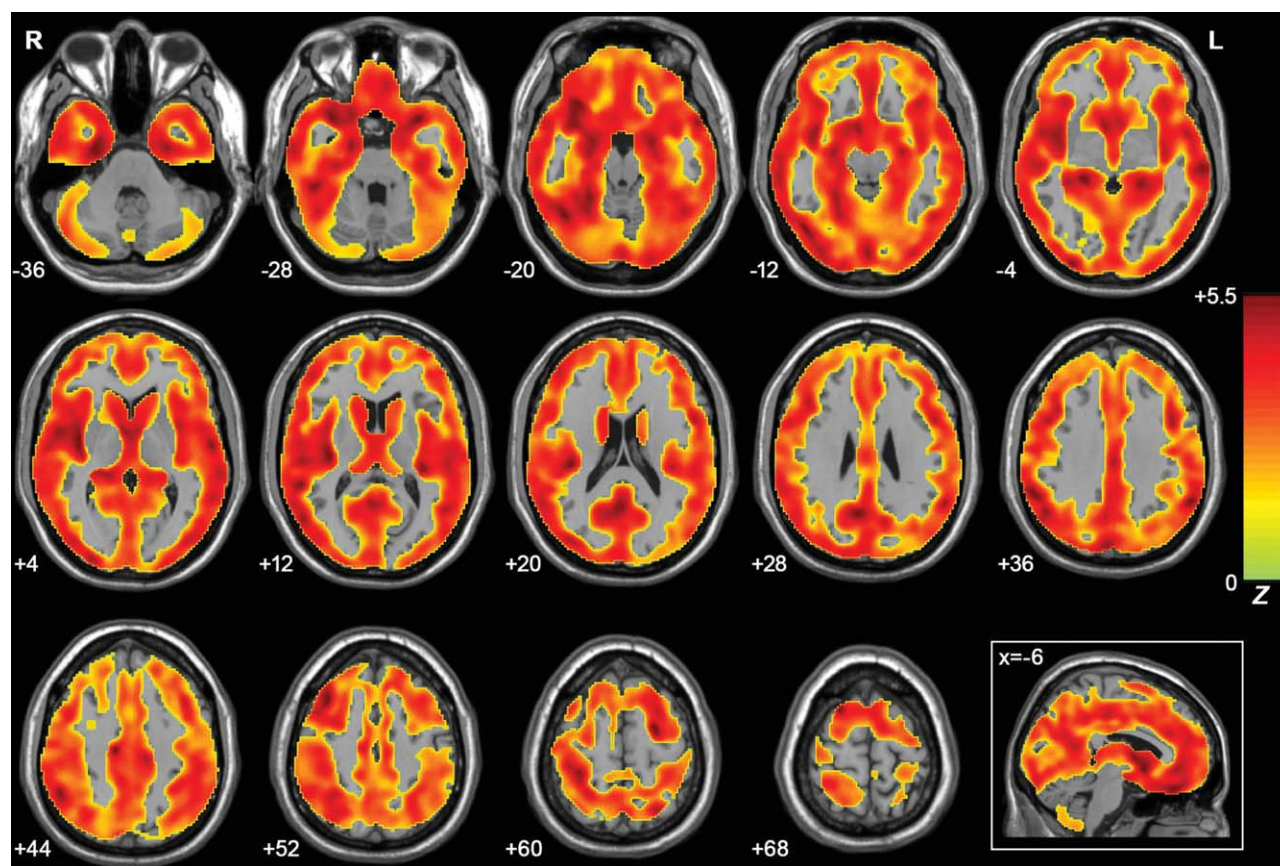
Figure 8.

Z-statistical maps of GM volume differences among the AD, MCI, and healthy elderly using a voxel-based-mophometry method. There were significant differences in the bilateral frontal, temporal, parietal, occipital lobe, and cerebellum. The statistical threshold was set at $|Z| > 1.96$ ($P < 0.05$) and cluster size $>1,404$ mm^3 (search volume: 1,575,720 mm^3), which corresponded to a corrected $P < 0.05$. [Color figure can be viewed in the online issue, which is available at wileyonlinelibrary.com.]

protocol has been used in many previous resting fMRI studies [Fox et al., 2005; Greicius et al., 2003; He et al., 2007; Zang et al., 2007]. However, there are also several researchers who have instructed their subjects to open their eyes during scans [Fox et al., 2005; Fransson, 2005]. Interestingly, two recent studies have reported that there were significant differences in the spontaneous brain activity between the eyes-closed and eyes-open conditions, and suggested that researchers should be cautious to choose between different resting conditions [Yan et al., 2009; Yang et al.,2007]. In future AD and MCI studies, it would be interesting to compare the results obtained under different resting-state conditions, and examine which condition could be more sensitive for detecting AD/MCI-associated changes in intrinsic brain activity. Second, the head motion of the participants may affect our results. Among the six translations and rotations parameters in x, y, or z directions, the mean z translation and roll rotation show signifi-

cant differences among the AD, MCI patients, and normal controls (Table VII). We also reanalyzed the data by taking the head-motion parameters as covariates, and found that the results remained nearly unchanged. It implies that our results of ALFF were not significantly influenced by the head motion. Third, this study compared relative ALFF changes in AD and MCI (see Methods). While analyzing raw ALFF values, we also revealed abnormal activities in many brain regions in AD and MCI (Supporting Information Fig. 1), which was approximately consistent with the relative ALFF results. Fourth, long-term physiological shifts and instrumental instability may contribute to a systematic increase or decrease in the signal with time [Lowe and Russell, 1999; Turner et al., 1997]. To reduce the effect, in this study, the linear trend was removed. In addition, the fMRI data is bandpass (0.01–0.08Hz) filtered to reduce the effects of very low frequency and high frequency physiological noise such as respiratory and aliased cardiac

TABLE VII. Head motion characteristics of the AD, MCI patients, and healthy controls

Head motion Characteristics	AD	MCI	Controls	P value
X translation (mm)	0.19 ± 0.16	0.14 ± 0.12	0.11 ± 0.10	0.20
Y translation (mm)	0.14 ± 0.08	0.17 ± 0.15	0.15 ± 0.12	0.78
Z translation (mm)	0.16 ± 0.08	0.27 ± 0.18	0.16 ± 0.10	0.02
Pitch (degree)	0.23 ± 0.22	0.32 ± 0.26	0.20 ± 0.21	0.26
Roll (degree)	0.24 ± 0.17	0.27 ± 0.22	0.12 ± 0.08	0.009
Yaw (degree)	0.24 ± 0.21	0.20 ± 0.14	0.13 ± 0.10	0.08

The P value was obtained by one-way analysis of variance test on head motion characteristics (mean absolute translation or rotation for each participant). Within the six translation and rotation parameters in x, y, or z directions, only the Z translation and roll rotation show significant ($P < 0.05$) differences among the AD, MCI, and control groups.

signals. It needs to be note that, according to the Nyquist-Shannon sampling theorem, the cardiac signals (usually 1.3Hz) can not be removed completely in the long TR (e.g., TR = 2 s) acquisition. However, it would be difficult to cover the whole brain if using a short TR (e.g., TR = 200 ms). Fifth, this study only examined the ALFF changes in AD and MCI patients. It would be interesting to ascertain whether the findings shown here are only specific to AD/MCI or might also be observed in other types of dementia such as vascular dementia, Lewy body dementia, and frontotemporal dementia. Further studies conducted on several different dementia groups would be helpful to clarify this issue. Finally, this study was cross-sectional. It has been suggested that about 50% of individuals with MCI develop AD. It would be important to explore changes in intrinsic brain activity between those who do and do not progress to AD, and to investigate longitudinal changes in MCI/AD subjects.

CONCLUSION

In this study, we found that AD and MCI patients showed abnormal ALFF in various brain regions of the frontal, temporal, and parietal lobes by examining intrinsic or spontaneous brain activity during rest. We demonstrated that the PCC showed the most significant group differences in ALFF, and the ALFF values in this region exhibited a general pattern of $ALFF_{AD} < ALFF_{MCI} < ALFF_{healthy\ elderly}$. Moreover, by using the ALFF for the PCC as an index, AD patients can be differentiated from healthy elderly with high sensitivity and specificity. Thus, this study offers insights into understanding the disease progression of the brain's intrinsic activities from healthy elderly to those with AD. In addition, our findings have implications for the understanding of the pathophysiology of dementia. Further work needs to be conducted to examine the developing progression of changes in intrinsic or

spontaneous brain activity by longitudinal studies of patients with AD and MCI.

REFERENCES

Allen G, Barnard H, McColl R, Hester AL, Fields JA, Weiner MF, Ringe WK, Lipton AM, Brooker M, McDonald E, Rubin CD, Cullum CM (2007): Reduced hippocampal functional connectivity in Alzheimer disease. Arch Neurol 64:1482–1487.

Allison T, Ginter H, McCarthy G, Nobre AC, Puce A, Luby M, Spencer DD (1994): Face recognition in human extrastriate cortex. J Neurophysiol 71:821–825.

American Psychiatric Association (1994): DSM-IV: Diagnostic and Statistical Manual of Mental Disorders, 4th ed. Washington, DC: American Psychiatric Association Press.

Anand A, Li Y, Wang Y, Wu J, Gao S, Bukhari L, Mathews VP, Kalnin A, Lowe MJ (2005): Activity and connectivity of brain mood regulating circuit in depression: A functional magnetic resonance study. Biol Psychiatry 57:1079–1088.

Ashburner J, Friston KJ (2005): Unified segmentation. Neuroimage 26:839–851.

Backman L, Andersson JL, Nyberg L, Winblad B, Nordberg A, Almkvist O (1999): Brain regions associated with episodic retrieval in normal aging and Alzheimer's disease. Neurology 52:1861–1870.

Bai F, Zhang Z, Yu H, Shi Y, Yuan Y, Zhu W, Zhang X, Qian Y (2008): Default-mode network activity distinguishes amnestic type mild cognitive impairment from healthy aging: A combined structural and resting-state functional MRI study. Neurosci Lett 438:111–115.

Baron JC, Chetelat G, Desgranges B, Perchey G, Landeau B, de la Sayette V, Eustache F (2001): In vivo mapping of gray matter loss with voxel-based morphometry in mild Alzheimer's disease. Neuroimage 14:298–309.

Becker JT, Mintun MA, Aleva K, Wiseman MB, Nichols T, DeKosky ST (1996): Compensatory reallocation of brain resources supporting verbal episodic memory in Alzheimer's disease. Neurology 46:692–700.

Biswal B, Yetkin FZ, Haughton VM, Hyde JS (1995): Functional connectivity in the motor cortex of resting human brain using echo-planar MRI. Magn Reson Med 34:537–541.

Bokde AL, Pietrini P, Ibanez V, Furey ML, Alexander GE, Graff-Radford NR, Rapoport SI, Schapiro MB, Horwitz B (2001): The effect of brain atrophy on cerebral hypometabolism in the visual variant of Alzheimer disease. Arch Neurol 58:480–486.

Bokde AL, Lopez-Bayo P, Meindl T, Pechler S, Born C, Faltraco F, Teipel SJ, Moller HJ, Hampel H (2006): Functional connectivity of the fusiform gyrus during a face-matching task in subjects with mild cognitive impairment. Brain 129:1113–1124.

Buckner RL, Snyder AZ, Shannon BJ, LaRossa G, Sachs R, Fotenos AF, Sheline YI, Klunk WE, Mathis CA, Morris JC, Mintun MA (2005): Molecular, structural, and functional characterization of Alzheimer's disease: Evidence for a relationship between

default activity, amyloid, and memory. J Neurosci 25:7709–7717.

Buckner RL, Andrews-Hanna JR, Schacter DL (2008): The brain's default network: Anatomy, function, and relevance to disease. Ann N Y Acad Sci 1124:1–38.

Buckner RL, Sepulcre J, Talukdar T, Krienen FM, Liu H, Hedden T, Andrews-Hanna JR, Sperling RA, Johnson KA (2009): Cortical hubs revealed by intrinsic functional connectivity: Mapping, assessment of stability, and relation to Alzheimer's disease. J Neurosci 29:1860–1873.

Castellanos FX, Margulies DS, Kelly C, Uddin LQ, Ghaffari M, Kirsch A, Shaw D, Shehzad Z, Di Martino A, Biswal B, Sonuga-Barke EJ, Rotrosen J, Adler LA, Milham MP (2008): Cingulate-precuneus interactions: A new locus of dysfunction in adult attention-deficit/hyperactivity disorder. Biol Psychiatry 63:332–337.

Collignon A, Maes F, Delaere D, Vandermeulen D, Suetens P, Marchal G (1995): Automated Multi-Modality Image Registration Based on Information Theory. Dordrecht, The Netherlands: Kluwer Academic Publishers. pp 263–274.

de Leon MJ, Convit A, Wolf OT, Tarshish CY, DeSanti S, Rusinek H, Tsui W, Kandil E, Scherer AJ, Roche A, Imossi A, Thorn E, Bobinski M, Caraos C, Lesbre P, Schlyer D, Poirier J, Reisberg B, Fowler J (2001): Prediction of cognitive decline in normal elderly subjects with 2-[(18)F]fluoro-2-deoxy-D-glucose/positron-emission tomography (FDG/PET). Proc Natl Acad Sci USA 98:10966–10971.

Dickerson BC, Bakkour A, Salat DH, Feczko E, Pacheco J, Greve DN, Grodstein F, Wright CI, Blacker D, Rosas HD, Sperling RA, Atri A, Growdon JH, Hyman BT, Morris JC, Fischl B, Buckner RL (2009): The cortical signature of Alzheimer's disease: Regionally specific cortical thinning relates to symptom severity in very mild to mild AD dementia and is detectable in asymptomatic amyloid-positive individuals. Cereb Cortex 19:497–510.

Fox MD, Raichle ME (2007): Spontaneous fluctuations in brain activity observed with functional magnetic resonance imaging. Nat Rev Neurosci 8:700–711.

Fox MD, Snyder AZ, Vincent JL, Corbetta M, Van Essen DC, Raichle ME (2005): The human brain is intrinsically organized into dynamic, anticorrelated functional networks. Proc Natl Acad Sci USA 102:9673–9678.

Fransson P (2005): Spontaneous low-frequency BOLD signal fluctuations: An fMRI investigation of the resting-state default mode of brain function hypothesis. Hum Brain Mapp 26:15–29.

Friston KJ, Frith CD, Frackowiak RS, Turner R (1995): Characterizing dynamic brain responses with fMRI: A multivariate approach. Neuroimage 2:166–172.

Garrity AG, Pearlson GD, McKiernan K, Lloyd D, Kiehl KA, Calhoun VD (2007): Aberrant "default mode" functional connectivity in schizophrenia. Am J Psychiatry 164:450–457.

Goldman RI, Stern JM, Engel J Jr, Cohen MS (2002): Simultaneous EEG and fMRI of the alpha rhythm. Neuroreport 13:2487–2492.

Gong G, He Y, Concha L, Lebel C, Gross DW, Evans AC, Beaulieu C (2009): Mapping anatomical connectivity patterns of human cerebral cortex using in vivo diffusion tensor imaging tractography. Cereb Cortex 19:524–536.

Good CD, Johnsrude IS, Ashburner J, Henson RN, Friston KJ, Frackowiak RS (2001): A voxel-based morphometric study of ageing in 465 normal adult human brains. Neuroimage 14:21–36.

Gould RL, Arroyo B, Brown RG, Owen AM, Bullmore ET, Howard RJ (2006): Brain mechanisms of successful compensation during learning in Alzheimer disease. Neurology 67:1011–1017.

Grady CL, McIntosh AR, Beig S, Keightley ML, Burian H, Black SE (2003): Evidence from functional neuroimaging of a compensatory prefrontal network in Alzheimer's disease. J Neurosci 23:986–993.

Greicius M (2008): Resting-state functional connectivity in neuropsychiatric disorders. Curr Opin Neurol 21:424–430.

Greicius MD, Krasnow B, Reiss AL, Menon V (2003): Functional connectivity in the resting brain: A network analysis of the default mode hypothesis. Proc Natl Acad Sci USA 100:253–258.

Greicius MD, Srivastava G, Reiss AL, Menon V (2004): Default-mode network activity distinguishes Alzheimer's disease from healthy aging: Evidence from functional MRI. Proc Natl Acad Sci USA 101:4637–4642.

Greicius MD, Flores BH, Menon V, Glover GH, Solvason HB, Kenna H, Reiss AL, Schatzberg AF (2007): Resting-state functional connectivity in major depression: Abnormally increased contributions from subgenual cingulate cortex and thalamus. Biol Psychiatry 62:429–437.

Gusnard DA, Raichle ME, Raichle ME (2001): Searching for a baseline: Functional imaging and the resting human brain. Nat Rev Neurosci 2:685–694.

Hagmann P, Cammoun L, Gigandet X, Meuli R, Honey CJ, Wedeen VJ, Sporns O (2008): Mapping the structural core of human cerebral cortex. PLoS Biol 6:e159.

Haxby JV, Ungerleider LG, Horwitz B, Maisog JM, Rapoport SI, Grady CL (1996): Face encoding and recognition in the human brain. Proc Natl Acad Sci USA 93:922–927.

Haxby JV, Gobbini MI, Furey ML, Ishai A, Schouten JL, Pietrini P (2001): Distributed and overlapping representations of faces and objects in ventral temporal cortex. Science 293:2425–2430.

He Y, Wang L, Zang Y, Tian L, Zhang X, Li K, Jiang T (2007): Regional coherence changes in the early stages of Alzheimer's disease: A combined structural and resting-state functional MRI study. Neuroimage 35:488–500.

He Y, Chen Z, Evans A (2008): Structural insights into aberrant topological patterns of large-scale cortical networks in Alzheimer's disease. J Neurosci 28:4756–4766.

Herholz K, Salmon E, Perani D, Baron JC, Holthoff V, Frolich L, Schonknecht P, Ito K, Mielke R, Kalbe E, Zundorf G, Delbeuck X, Pelati O, Anchisi D, Fazio F, Kerrouche N, Desgranges B, Eustache F, Beuthien-Baumann B, Menzel C, Schroder J, Kato T, Arahata Y, Henze M, Heiss WD (2002): Discrimination between Alzheimer dementia and controls by automated analysis of multicenter FDG PET. Neuroimage 17:302–316.

Hoptman MJ, Zuo XN, Butler PD, Javitt DC, D'Angelo D, Mauro CJ, Milham MP (2010): Amplitude of low-frequency oscillations in schizophrenia: A resting state fMRI study. Schizophr Res 117:13–20.

Horwitz B, McIntosh AR, Haxby JV, Furey M, Salerno JA, Schapiro MB, Rapoport SI, Grady CL (1995): Network analysis of PET-mapped visual pathways in Alzheimer type dementia. Neuroreport 6:2287–2292.

Johnson SC, Saykin AJ, Baxter LC, Flashman LA, Santulli RB, McAllister TW, et al. (2000): The relationship between fMRI activation and cerebral atrophy: Comparison of normal aging and Alzheimer disease. NeuroImage 11:179–187.

Kanwisher N, McDermott J, Chun MM (1997): The fusiform face area: A module in human extrastriate cortex specialized for face perception. J Neurosci 17:4302–4311.

Kiviniemi V, Jauhiainen J, Tervonen O, Paakko E, Oikarinen J, Vainionpaa V, Rantala H, Biswal B (2000): Slow vasomotor fluctuation in fMRI of anesthetized child brain. Magn Reson Med 44:373–378.

Kohler S, McIntosh AR, Moscovitch M, Winocur G (1998): Functional interactions between the medial temporal lobes and posterior neocortex related to episodic memory retrieval. Cereb Cortex 8:451–461.

Ledberg A, Akerman S, Roland PE (1998): Estimation of the probabilities of 3D clusters in functional brain images. Neuroimage 8:113–128.

Lerch JP, Pruessner JC, Zijdenbos A, Hampel H, Teipel SJ, Evans AC (2005): Focal decline of cortical thickness in Alzheimer's disease identified by computational neuroanatomy. Cereb Cortex 15:995–1001.

Li SJ, Li Z, Wu G, Zhang MJ, Franczak M, Antuono PG (2002): Alzheimer Disease: Evaluation of a functional MR imaging index as a marker. Radiology 225:253–259.

Liang M, Zhou Y, Jiang T, Liu Z, Tian L, Liu H, Tian L, Liu H, Hao Y (2006): Widespread functional disconnectivity in schizophrenia with resting-state functional magnetic resonance imaging. Neuroreport 17:209–213.

Logothetis NK, Pauls J, Augath M, Trinath T, Oeltermann A (2001): Neurophysiological investigation of the basis of the fMRI signal. Nature 412:150–157.

Lowe MJ, Mock BJ, Sorenson JA (1998): Functional connectivity in single and multislice echoplanar imaging using resting-state fluctuations. Neuroimage 7:119–132.

Lowe MJ, Russell DP (1999): Treatment of baseline drifts in fMRI time series analysis. J Comput Assist Tomogr 23:463–473.

Lowe MJ, Phillips MD, Lurito JT, Mattson D, Dzemidzic M, Mathews VP (2002): Multiple sclerosis: Low-frequency temporal blood oxygen level-dependent fluctuations indicate reduced functional connectivity initial results. Radiology 224:184–192.

Lu H, Zuo Y, Gu H, Waltz JA, Zhan W, Scholl CA, Rea W, Yang Y, Stein EA (2007): Synchronized delta oscillations correlate with the resting-state functional MRI signal. Proc Natl Acad Sci USA 104:18265–18269.

Lui S, Huang X, Chen L, Tang H, Zhang T, Li X, Li D, Kuang W, Chan RC, Mechelli A, Sweeney JA, Gong Q (2009): High-field MRI reveals an acute impact on brain function in survivors of the magnitude 8.0 earthquake in China. Proc Natl Acad Sci USA 106:15412–15417..

Lustig C, Snyder AZ, Bhakta M, O'Brien KC, McAvoy M, Raichle ME, Morris JC, Buckner RL (2003): Functional deactivations: Change with age and dementia of the Alzheimer type. Proc Natl Acad Sci USA 100:14504–14509.

Maxim V, Sendur L, Fadili J, Suckling J, Gould R, Howard R, Bullmore E (2005): Fractional Gaussian noise, functional MRI and Alzheimer's disease. Neuroimage 25:141–158.

McKhann G, Drachman D, Folstein M, Katzman R, Price D, Stadlan EM (1984): Clinical diagnosis of Alzheimer's disease: Report of the NINCDS-ADRDA Work Group under the auspices of Department of Health and Human Services Task Force on Alzheimer's Disease. Neurology 34:939–944.

Moosmann M, Ritter P, Krastel I, Brink A, Thees S, Blankenburg F, Taskin B, Obrig H, Villringer A (2003): Correlates of alpha rhythm in functional magnetic resonance imaging and near infrared spectroscopy. Neuroimage 20:145–158.

Morris JC (1993): The clinical dementia rating (CDR): Current version and scoring rules. Neurology 43:2412–2414.

Oakes TR, Fox AS, Johnstone T, Chung MK, Kalin N, Davidson RJ (2007): Integrating VBM into the general linear model with voxelwise anatomical covariates. Neuroimage 34:500–508.

Petersen RC, Smith GE, Waring SC, Ivnik RJ, Tangalos EG, Kokmen E (1999): Mild cognitive impairment: clinical characterization and outcome. Arch Neurol 56:303–308.

Prvulovic D, Hubl D, Sack AT, Melillo L, Maurer K, Frolich L, Lanfermann H, Zanella FE, Goebel R, Linden DE, Dierks T (2002): Functional imaging of visuospatial processing in Alzheimer's disease. Neuroimage 17:1403–1414.

Raichle ME, MacLeod AM, Snyder AZ, Powers WJ, Gusnard DA, Shulman GL (2001): A default mode of brain function. Proc Natl Acad Sci USA 98:676–682.

Salmon E, Collette F, Degueldre C, Lemaire C, Franck G (2000): Voxel-based analysis of confounding effects of age and dementia severity on cerebral metabolism in Alzheimer's disease. Hum Brain Mapp 10:39–48.

Saykin AJ, Flashman LA, Frutiger SA, Mamourian AC, Moritz CH, O'Jile JR, Riordan HJ, Santulli RB, Smith CA, Weaver JB (1999): Neuroanatomic substrates of semantic memory impairment in Alzheimer's disease: Patterns of functional MRI activation. J Int Neuropsychol Soc 5:377–392.

Shmuel A, Leopold DA (2008): Neuronal correlates of spontaneous fluctuations in fMRI signals in monkey visual cortex: Implications for functional connectivity at rest. Hum Brain Mapp 29:751–761.

Singh V, Chertkow H, Lerch JP, Evans AC, Dorr AE, Kabani NJ (2006): Spatial patterns of cortical thinning in mild cognitive impairment and Alzheimer's disease. Brain 129:2885–2893.

Sorg C, Riedl V, Muhlau M, Calhoun VD, Eichele T, Laer L, Drzezga A, Forstl H, Kurz A, Zimmer C, Wohlschlager AM (2007): Selective changes of resting-state networks in individuals at risk for Alzheimer's disease. Proc Natl Acad Sci USA 104:18760–18765.

Tian L, Jiang T, Wang Y, Zang Y, He Y, Liang M, Sui M, Cao Q, Hu S, Peng M, Zhuo Y (2006): Altered resting-state functional connectivity patterns of anterior cingulate cortex in adolescents with attention deficit hyperactivity disorder. Neurosci Lett 400:39–43.

Turner R, Howseman A, Rees G, Josephs O (1997): Functional imaging with magnetic resonance. In: Frackowiak, R.S.J. (Ed.), Human Brain Function. Academic Press, San Diego, pp. 467–486.

Tzourio-Mazoyer N, Landeau B, Papathanassiou D, Crivello F, Etard O, Delcroix N, Mazoyer B, Joliot M (2002): Automated anatomical labeling of activations in SPM using a macroscopic anatomical parcellation of the MNI MRI single-subject brain. Neuroimage 15:273–289.

Volkow ND, Zhu W, Felder CA, Mueller K, Welsh TF, Wang GJ, de Leon MJ (2002): Changes in brain functional homogeneity in subjects with Alzheimer's disease. Psychiatry Res 114:39–50.

Wang L, Zang Y, He Y, Liang M, Zhang X, Tian L, Wu T, Jiang T, Li K (2006): Changes in hippocampal connectivity in the early stages of Alzheimer's disease: Evidence from resting state fMRI. Neuroimage 31:496–504.

Wang K, Liang M, Wang L, Tian L, Zhang X, Li K, Jiang T (2007): Altered functional connectivity in early Alzheimer's disease: A resting-state fMRI study. Hum Brain Mapp 28:967–978.

Yan C, Zang Y (2010): DPARSF: A MATLAB toolbox for "pipe-line" data analysis of resting-state fMRI. Front Syst Neurosci 4:13.

Yan C, Liu D, He Y, Zou Q, Zhu C, Zuo X, Long X, Zang Y (2009): Spontaneous brain activity in the default mode network is sensitive to different resting-state conditions with limited cognitive load. PLoS ONE 4:e5743.

Yang H, Long XY, Yang Y, Yan H, Zhu CZ, Zhou XP, Zang YF, Gong QY (2007): Amplitude of low frequency fluctuation within visual areas revealed by resting-state functional MRI. Neuroimage 36:144–152.

Yetkin FZ, Rosenberg RN, Weiner MF, Purdy PD, Cullum CM (2006): FMRI of working memory in patients with mild cognitive impairment and probable Alzheimer's disease. Eur Radiol 16:193–206.

Zang YF, He Y, Zhu CZ, Cao QJ, Sui MQ, Liang M, Tian LX, Jiang TZ, Wang YF (2007): Altered baseline brain activity in children with ADHD revealed by resting-state functional MRI. Brain Dev 29:83–91.

Zhang HY, Wang SJ, Xing J, Liu B, Ma ZL, Yang M, Zhang ZJ, Teng GJ (2009): Detection of PCC functional connectivity characteristics in resting-state fMRI in mild Alzheimer's disease. Behav Brain Res 197:103–108.